Investigations on the Q and CT Bands of Cytochrome *c* Submonolayer Adsorbed on an Alumina Surface Using Broadband Spectroscopy with Single-Mode Integrated Optical Waveguides

Rodrigo S. Wiederkehr,[†] Geoffrey C. Hoops,[‡] Mustafa M. Aslan,[†] Courtney L. Byard,[†] and Sergio B. Mendes*,[†]

Department of Physics and Astronomy, University of Louisville, Louisville, Kentucky 40292, Department of Chemistry, Butler University, 4600 Sunset Avenue, Indianapolis, Indiana 46208

Received: December 9, 2008; Revised Manuscript Received: March 21, 2009

In this work, we report experimental results on the molar absorptivity of cytochrome *c* adsorbed at different submonolayer levels onto an aluminum oxide waveguide surface; our data show a clear dependence of the protein optical properties on its surface density. The measurements were performed using the broadband, single-mode, integrated optical waveguide spectroscopic technique, which is an extremely sensitive tool able to reach submonolayer levels of detection required for this type of studies. This investigation focuses on the molar absorptivity at the Q-band (centered at 525 nm) and, for the first time to our knowledge, the weak charge transfer (CT) band (centered at 695 nm) of surface-adsorbed cyt *c*. Polarized light in the spectral region from 450 to 775 nm was all-coupled into an alumina thin film, which functioned as a single-mode planar optical waveguide. The alumina thin-film waveguide used for this work had a thickness of 180 nm and was deposited on a glass substrate by the atomic layer deposition process. The protein submonolayer was formed on the alumina waveguide surface through electrostatic adsorption from an aqueous buffer solution at neutral pH. The optical properties of the surface-adsorbed cyt *c* were investigated for bulk protein concentrations ranging from 5 nM to 8200 nM in the aqueous buffer solution. For a protein surface density of 2.3 pmol/cm^2, the molar absorptivity measured at the charge transfer band was 335 M^{-1} cm^{-1}, and for a surface density of 15 pmol/cm^2 was 720 M^{-1} cm^{-1}, which is much closer to the value of cyt *c* dissolved in an aqueous neutral buffer (830 M^{-1} cm^{-1}). The modification of the protein molar absorptivity and its dependence on the surface density can most likely be attributed to conformational changes of the surface-adsorbed species.

1. Introduction

Protein adsorption is a process that occurs spontaneously whenever a protein dissolved in aqueous solutions contacts a solid surface, resulting in modification of the surface and often conformational changes in the protein, as well.[1] It is a topic of increasing interest because of its importance in biosensors,[2] chromatography,[3] biocompatibility,[4] and in many other biotechnology applications. The surface interaction may alter some of the protein properties, such as the molar absorptivity, due to surface-induced conformational changes[5,6] resulting from a combination of short-range (van der Waals, hydrogen bonding) and long-range (electrostatic attraction/repulsion) interactions. Globular proteins are highly ordered structures of low entropy that upon adsorption may (partly) increase their entropy under conformational changes.[7] This entropy gain may be also sufficiently large to contribute to spontaneous adsorption under adverse conditions, such as on an electrostatically repelling surface.[8]

Broadband absorbance spectroscopy with single-mode integrated optical waveguides is a highly sensitive technique for detecting surface-adsorbed molecules[9−12] due to the long and strong optical interaction of surface-bound chromophores with the evanescent field that emerges from a guiding thin film wherein the propagating light is mostly confined.[13] When compared to the traditional direct transmission mode or attenuated total reflection (ATR) technique, the major advantage of using a single-mode optical waveguide platform lies in the much enhanced effective path length of the single-mode waveguide for interrogating surface-adsorbed chromophores. The value of the sensitivity enhancement factor, usually defined as the ratio of the absorbance measured with a waveguide platform divided by the absorbance measured in direct transmission, can be 4−5 orders of magnitude for a single-mode integrated optical waveguide.[13] Broadband waveguide couplers[9,12,14,15] have enabled spectroscopic capability to the single-mode integrated optical waveguide technique, which then has been demonstrated to be a powerful tool for optical investigations of surface-bound biomolecular materials at the submonolayer regime. The polarized absorbance data measured with a waveguide-based platform can then be directly related to the spectroscopic properties (molar absorptivity) of the molecular layer under investigation.[16]

Cytochrome *c* is a small electron transfer protein which has been used in several research works due to commercially availability of large amounts in relatively pure form. The absorbance spectral properties of this protein in solution has already been extensively studied.[17] The strong absorbance peak at 409 nm (Soret band with molar absorptivity of 106 000 M^{-1} cm^{-1}) and two other relatively weak absorbance peaks at 525 nm (Q-band with molar absorptivity of 10 600 M^{-1} cm^{-1}) and 695 nm (charge transfer band with molar absorptivity of 830 M^{-1} cm^{-1}) for the protein dissolved in neutral buffer solution (pH = 7.2) have collectively been used to study conformational

* Corresponding author. Phone: +1 502 852-0908. Fax: +1 502 852-8128. E-mail: sbmend01@louisville.edu.
[†] University of Louisville.
[‡] Butler University.

10.1021/jp810845e CCC: $40.75
Published on Web 04/20/2009

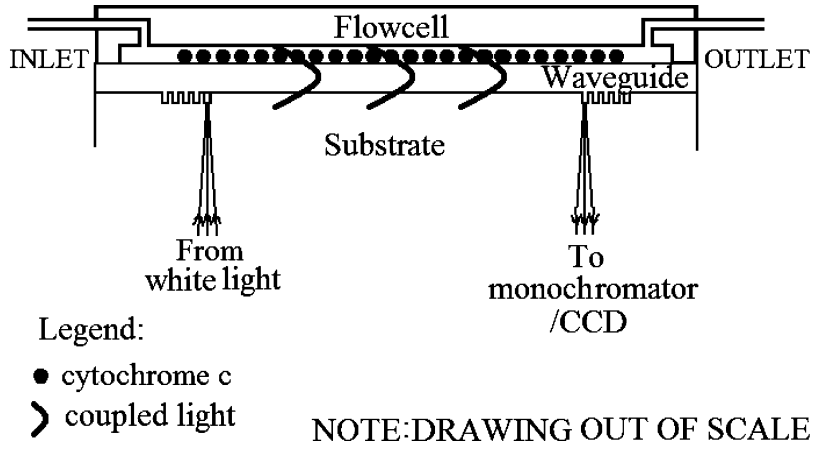

Figure 1. Schematic drawing of the waveguide from the lateral view with the flowcell mounted on the top surface. The black dots represent the protein adsorbed to the surface. The light with TE polarization was coupled to the waveguide by the diffraction gratings patterned in the substrate.

changes due to pH changes of the buffer[18,19] (denaturation) or temperature[20] or addition of ligands such as cyanide,[21] azide,[22] or imidazole.[23] However, there are few reports in the literature describing possible conformational changes for cytochrome *c* adsorbed to a surface because of the difficulty of measuring the absorbance by a thin layer of protein attached to a surface. Santos et al.[24] used an ATR technique in silica slides (0.1 mm) to study the adsorption of cytochrome *c* dissolved in phosphate buffer at variable pH. The influence of the bulk protein concentration to the isotherm adsorption curves was reported; from these data, the authors suggested that the area occupied by individual protein molecules on the silica surface is dependent upon the protein concentration in the bulk solution. Edmiston et al.[25] used monochromatic light measurements with integrated optical waveguide and total internal reflection fluorescence to investigate molecular orientation of cytochrome *c* adsorbed to hydrophobic and hydrophilic surfaces.

In this work, we present the experimental results obtained using our single-mode optical waveguide spectrometer for the molar absorptivity of oxidized cytochrome *c* immobilized onto an alumina surface. The alumina material was chosen for the guiding film because it provides single-mode integrated optical waveguides with very low optical losses over a broad spectral range and has a high refractive index that highly confines the optical field for a sensitive detection of surface-adsorbed chromophores. The extremely high sensitivity of our instrument allowed the observation of cytochrome *c*'s Q and charge transfer bands while the protein was adsorbed to an aluminum oxide surface at submonolayer levels. The results obtained on the alumina waveguide surface were compared with corresponding values in solution, obtained using conventional spectroscopy. Furthermore, it was possible to relate spectral changes of the adsorbed species to the different surface coverage of the protein on the waveguide surface. Our measurements clearly show that the molar absorptivity is dependent upon the surface coverage.

2. Experimental Procedures

Oxidized Cytochrome *c* Preparation. Horse heart cytochrome *c* was obtained commercially (Sigma-Aldrich) and dialyzed extensively against 10 mM NaCl at 25 °C.[26] The final concentration of the stock solution was determined using the molar absorptivity peak of the Soret band (409 nm) for the oxidized cytochrome *c* ($\varepsilon_{409} = 106\,000\ M^{-1}\ cm^{-1}$).[27] To obtain solutions with concentrations ranging from [cyt *c*] = 5 nM to 8200 nM, the stock solution was diluted in 7 mM sodium phosphate with 10 mM NaCl (pH = 7.2).

Optical Waveguide Spectroscopy of Cytochrome *c*. The single-mode, integrated optical waveguide spectrometer used for the data reported in this study was developed in our laboratories at the University of Louisville on the basis of previous work reported in the literature,[10,12−15] and details of the working principles of the instrumentation were already discussed elsewhere.[13,28] The setup used is composed of a light source, a single-mode planar optical waveguide with integrated grating couplers, a flowcell, a monochromator, and a charge-couple device (CCD) array detector. The light source used was a white lamp (Philips, FocusLine 6 V) with spectral emission from 430 to 800 nm. To couple broadband light into the waveguide, two diffraction gratings positioned 3.4 cm distant from each other were microfabricated into the glass substrate. For this purpose, a photoresist film (Shipley 1805) was photopatterned by a holographic technique, and after exposure and development of the holographic pattern, a reactive ion-etching process was performed to transfer the periodic modulation in the photoresist film onto the surface of the glass slide substrate.[29] The grating period fabricated for this work was approximately 400 nm so that the center wavelength of light coupled to the waveguide was about 600 nm and the coupled band spanned from 460 to 740 nm. Glass substrates with a pair of diffraction gratings were coated with an aluminum oxide layer by the atomic layer deposition technique (Cambridge Nanotech); the alumina thin film was chosen as a dielectric confining waveguide due to its high refractive index and low propagation loss (less than 1 dB/cm) over a broad spectral range. The precursors used in the atomic layer deposition technique for the alumina deposition were trimethylalumium and water. These precursors were injected in a pulsed manner into the deposition chamber to react with each other near the substrate and create a film upon the surface. The parameters of the deposition (number of pulses and substrate temperature) were adjusted to obtain a film with thickness of about $t = 180$ nm to function as a single-mode, planar optical waveguide. A linear polarizer was placed in the optical path to allow for only the transverse electric (TE) light modes to couple into the waveguide and provide a basis for unequivocal analysis of protein properties, such as surface coverage and molar absorptivity. To adsorb the protein to the waveguide surface, a flowcell with volume of ~2 mL was attached to the top of the waveguide surface. Figure 1 shows a schematic drawing of the waveguide with a flowcell.

The out-coupled light beam was fiber-guided to a monochromator (SpectraPro 2300, Acton-Princeton) that dispersed light into the CCD (Pixis 400, Princeton) detector. The CCD is composed of an array of pixels (1340 × 400), and each column in the detector is associated with a specific wavelength. The number of counts on each pixel was measured after a certain acquisition time. For each experiment, a baseline signal was initially acquired with just buffer in the flowcell, and then, after protein adsorption to the waveguide surface from the buffer solution, sequential acquisitions were performed. Those data allowed us to calculate the absorbance, surface density, and molar absorptivity that are presented in the results section. All the data acquisitions were performed at room temperature (25 °C).

Measurement Of protein in Solution. The concentration of cytochrome *c* for all solutions used in this experiment were directly determined by absorbance at the Soret peak (409 nm), as measured in a quartz cuvette using a spectrophotometer Cary 300 (Varian). The molar absorptivity of cytochrome *c* in solution at 409 nm is known (ε_{409} = 106 000 M^{-1} cm^{-1}),[27] so the concentration was determined using Beer's law. The bulk solution concentration for the protein was measured after passage through the flowcell of the waveguide spectrometer. All the concentration measurements were performed at room temperature (25 °C).

3. Results and Discussions

Sensitivity of the Single-Mode Waveguide Spectrometer. The sensitivity factor, *S*, defined as the ratio between the waveguide absorbance, A_{WG}, and the direct transmission absorbance, $A_{TR} = \varepsilon_{surf}\ \Gamma$, is described by the following relation,[13,28]

$$S = \frac{A_{WG}}{\varepsilon_{surf}\Gamma} \tag{1}$$

where ε_{surf} is the molar absorptivity of the surface-bound protein and Γ is the protein surface density. The sensitivity factor is a key variable to determine the limit of detection of a waveguide-based spectrometer because a higher sensitivity factor translates into a higher absorbance value for a given chromophore at a certain surface density. For a waveguide mode at the TE polarization, the sensitivity factor can be described by the following equation,[28]

$$S_{TE} = \frac{2n_l(n_w^2 - N_{TE}^2)}{N_{TE}(n_w^2 - n_c^2)}\frac{L}{t_{eff,TE}} \tag{2}$$

where n_l is the real part of the refractive index of the adsorbed protein monolayer, n_w is the refractive index of the alumina guiding film, n_c is the refractive index of the buffer solution, N_{TE} is the effective index of the waveguide, $t_{eff,TE}$ is the effective thickness of the waveguide (which is related to physical thickness of the guiding film, *t*), and *L* is the distance between the input and output couplers. For the single-mode, alumina-thin-film waveguide used in this work, the sensitivity factor is presented in Figure 2 as a function of the wavelength; the results in this plot were obtained by using eqs 1 and 2 at each wavelength. For the application of those equations, we experimentally determined that the refractive index of the alumina waveguide thin film can be described by: $n_w = a + (b)/(\lambda^2) + (c)/(\lambda^4)$, where a = 1.645 76, b = 42.898 98, and c = 308 958 233.142. For the refractive index of the aqueous buffer solution, we used n_c = 1.33, and the approximation[30] that $n_l \approx n_c$. As previously mentioned, the thickness of the guiding film is given by t = 180 nm, and the distance between the input and output couplers is L = 3.4 cm. The effective refractive index, N_{TE}, and the effective thickness, $t_{eff,TE}$, were calculated from the waveguide dispersion equation (with n_s = 1.51).[16] As seen in Figure 2, at the 525-nm (Q-band), the waveguide spectrometer is about 38 000 times more sensitive than an absorbance measurement in direct transmission.

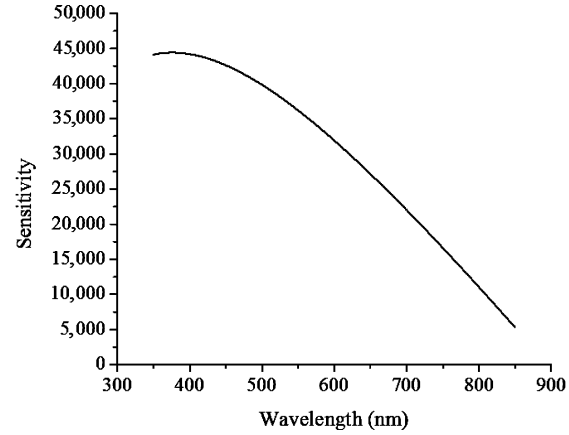

Figure 2. Sensitivity values as function of light wavelength for an alumina waveguide with 180 nm of thickness and a propagation length of 3.4 cm.

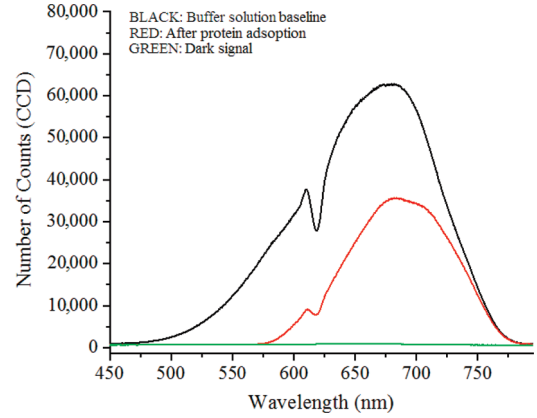

Figure 3. Light intensity against wavelength measured with the single-mode waveguide spectrometer at different steps of an experiment to determine the optical absorbance spectrum of a protein film.

Absorbance of Cytochrome *c* Adsorbed to an Aluminum Oxide Waveguide. To obtain the absorbance of cytochrome *c* adsorbed to the waveguide surface, we converted the number of counts acquired by the CCD from the out-coupled light of the waveguide spectrometer into absorbance units. In all measurements, the exposure time was fixed to 30 s. In Figure 3, we illustrate a typical sequence of measurements that was used to obtain an absorbance spectrum with our waveguide-based spectrometer. The black curve corresponds to an intensity measurement with just buffer solution (7 mM phosphate buffer with 10 mM NaCl at pH 7.2) inside the flowcell. The red curve corresponds to an intensity measurement with a protein solution of 8200 nM inside the flowcell after an incubation time of 50 min. A straightforward calculation[28] can show that the contribution from the dissolved species is negligible; thus, the intensity measured is essentially due to the protein molecules adsorbed onto the waveguide surface. The green curve corresponds to the case in which the waveguide signal was completely attenuated by crossing the input and output polarizers. From those measurements, the absorbance spectrum of the protein film was then obtained by the following equation:

$$A = -\log_{10}\left(\frac{C_{\text{cyt}\,c} - C_{\text{dark}}}{C_{\text{buffer}} - C_{\text{dark}}}\right) \quad (3)$$

where A is the absorbance, $C_{\text{cyt}\,c}$ is the number of counts measured for cytochrome *c* adsorbed to the waveguide surface, C_{buffer} is the number of counts for the buffer, and C_{dark} is the number of counts for the absence of out-coupling light (dark signal).

In this work, spectra were acquired for cytochrome *c* with bulk solution concentrations ranging from 5 nM to 8200 nM. At each concentration, measurements were performed every 5 min after injection of the protein solution into the flowcell and until equilibrium was reached with no further changes observed in the protein spectra. In Figure 4(a), absorbance spectra of adsorbed cytochrome *c* at equilibrium for different bulk solution concentrations are presented; in Figure 4(b) the 695 nm spectral region is magnified to better visualize the charge transfer band. These results showcase the extremely high sensitivity of our single-mode, waveguide-based spectrometer that can measure even very weak absorption peaks, such as the charge transfer band, for a protein adsorbed to a surface.

To visualize possible concentration-dependent changes in the cyt *c* spectra near the 695 nm region, a straight line was subtracted from the charge transfer peak.[31] Figure 5(a) illustrates how the subtraction was performed, and in Figure 5(b) the subtracted absorption spectra for the different cytochrome *c* concentrations are plotted together. The absorbance peak for the CT band remains centered at approximately 695 nm, because there are at best only minimal expressive shifts (red or blue) in the spectra resulting from variable cytochrome *c* concentrations ranging from undetectable adsorption levels to saturation levels (~700 nM) on the alumina waveguide surface.

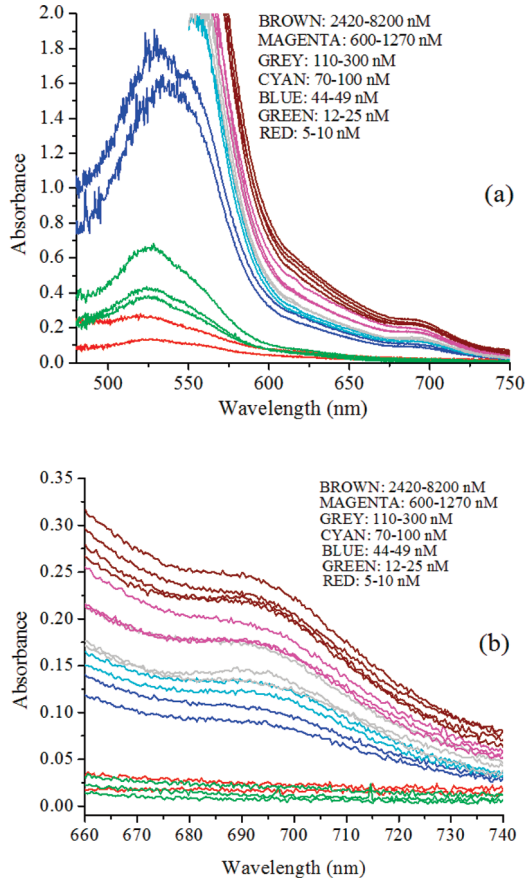

Figure 4. (a) Absorbance for cytochrome *c* adsorbed to the alumina waveguide surface at different concentrations. (b) Magnified view of the charge transfer band. The legends show the protein concentration in the bulk solution measured after being adsorbed to the waveguide surface.

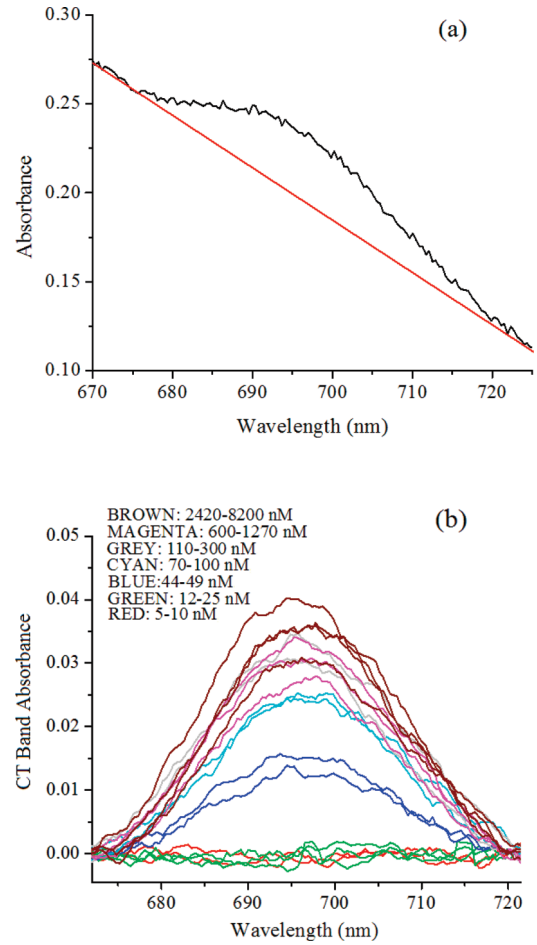

Figure 5. (a) Example of straight line subtraction from the charge transfer absorption band. (b) Absorbance of the CT band after straight-line subtraction for variable solution concentrations of cytochrome *c*.

Adsorption Isotherm. To calculate the surface density of the protein film, we solved eq 1 for Γ and employed the experimental results of the absorbance, $A_{\text{WG,TE}}$, measured by our single-mode-based waveguide spectrometer and the results of the sensitivity factor, S_{TE}, from eq 2, which were already described in Figure 2. In addition, the results from Figure 5 that the CT absorption band of cytochrome *c* adsorbed to the waveguide surface is similar to those of the dissolved in buffer solution allowed us to assume that

$$\varepsilon_{\text{surf}}(\lambda) = \varepsilon_{\text{sol}}(\lambda) \quad (4)$$

for the region of 725−740 nm of the spectra. The molar absorptivity of cytochrome *c* in solution for the 725−740 nm region is a smooth curve with low values tending to zero, the same as observed for the cytochrome adsorbed to the waveguide surface; thus, this assumption seems to be a good approximation. Nonetheless, later in this article, we will revisit this assumption. The surface packing density was then calculated at several wavelengths in the 725−740 nm region using the equation

$$\Gamma = \frac{A_{\text{WG,TE}}}{S_{\text{TE}}\varepsilon_{\text{surf}}} \quad (5)$$

From the several values obtained for Γ, an average value was determined. Such redundancy and averaging process in the

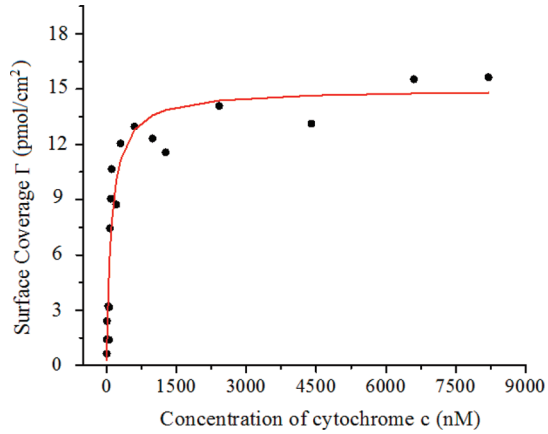

Figure 6. Surface coverage for cytochrome *c* adsorbed on an alumina waveguide surface for different bulk concentrations. An adsorption equilibrium constant, K_{ad}, of $(10 \pm 2) \times 10^6$ M^{-1} was determined from our experimental results.

determination of Γ are quite helpful in minimizing experimental errors. The surface coverage for different concentrations of cytochrome *c* in the buffer solution is presented in Figure 6; the solution concentration ranged from 5 to 8200 nM. For the purpose of fitting our experimental data, we included in Figure 6 a Langmuir isotherm curve described by

$$\Gamma = \frac{K_{ad}\Gamma_{max}C}{1 + K_{ad}C} \tag{6}$$

where Γ is the surface packing density, K_{ad} is the adsorption equilibrium constant, Γ_{max} is the maximum amount adsorbed, and C_b is the protein concentration in bulk solution. Cytochrome *c* appears to be forming a monolayered film on the waveguide alumina surface with a maximum surface packing density of (15 ± 1) pmol/cm^2. This maximum surface packing density is higher than that previously observed on glass,[32] but lower than that observed on silica[26] and indium tin oxide[32,33] bare surfaces. The adsorption equilibrium constant, K_{ad}, obtained from the Langmuir fitting, $K_{ad} = (10 \pm 2) \times 10^6$ M^{-1}, is also largely consistent with that observed for cytochrome *c* on bare silica,[26] $(12 \pm 2) \times 10^6$ M^{-1}, and bare indium tin oxide,[33] $(20 \pm 8) \times 10^6$ M^{-1}, under similar conditions.

Molar Absorptivity of Cytochrome *c* Adsorbed onto an Aluminum Oxide Surface. The molar absorptivity is a measurement of the amount of light absorbed by a particular chromophore and is generally independent of the chromophore concentration. However, if the protein is adsorbed to a surface, the surface environment may affect the molecular structure with possible consequences on the spectral profile of the molar absorptivity; in addition, the molecular surface coverage may also affect the optical properties. To obtain the molar absorptivity, for the adsorbed cytochrome *c* across the spectral range available from our experimental data, we employed eq 1 and the results obtained in the last section for the surface density at different protein concentrations in the bulk solution. Figure 7(a) and (b) presents the results obtained for the molar absorptivity at different surface densities in the protein film. In Figure 7(a), the molar absorptivity at the Q-band (525 nm) is presented only for low surface densities because the absorbance reaches excessive values at higher surface density concentrations. For comparison, we included the molar absorptivity obtained for cyt *c* in buffer solution (black curve) using a standard UV−vis spectrophotometer (Cary 300), and these data agree very well with literature values.[17] However, from Figure 7(a) and (b), our

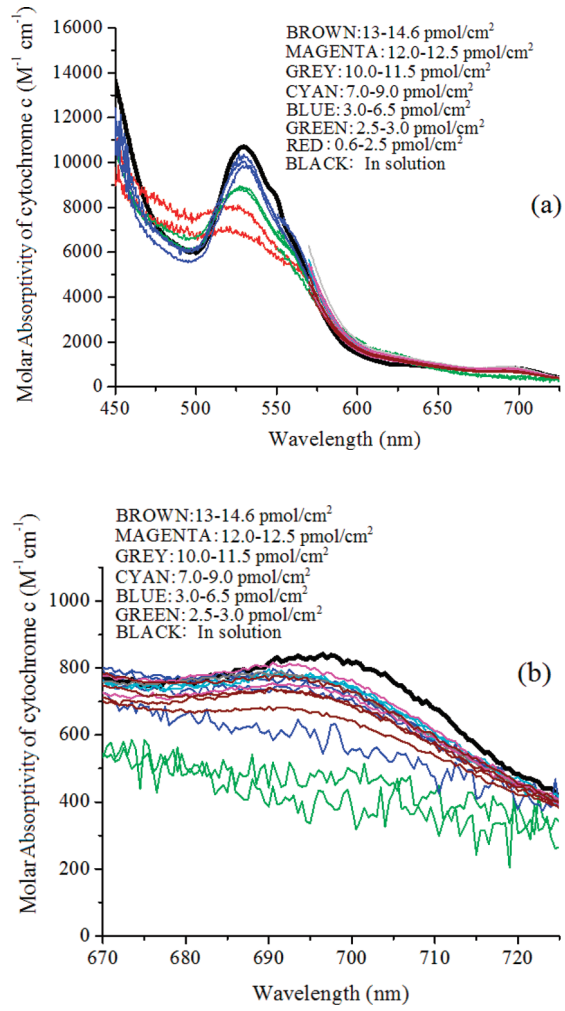

Figure 7. (a) Molar absorptivity for cytochrome *c* adsorbed to an aluminum oxide surface. The curves represent different surface densities calculated for the different concentrations in bulk solution. (b) Magnified view of the 670−720 nm region to better visualize the CT band.

data show that the molar absorptivity of cytochrome *c* adsorbed to an aluminum oxide surface changes its spectral profile when compared to the protein dissolved in buffer solution. In addition, we notice that the surface coverage affects the results of the molar absorptivity. For a surface coverage of 2.3 pmol/cm^2, the value measured for the molar absorptivity at the charge transfer band (695 nm) was 335 M^{-1} cm^{-1}. However, for a surface almost fully covered (gray curves with surface coverage of 11 pmol/cm^2), we measured 775 M^{-1} cm^{-1}, which approximates the value for the protein freely dissolved in solution (830 M^{-1} cm^{-1}).

Additional measurements were performed to ensure that these observed changes were, indeed, due to the different environments to which the protein is exposed (aqueous solution versus alumina waveguide surface) and not to an instrumental artifact. For this verification, the molar absorptivity of cytochrome *c* dissolved in a buffer solution was measured both in our waveguide-based instrument (placing a 1 cm cuvette in the optical path) and in the Cary 300 spectrophotometer. The results shown in Figure 8 are quite close and rule out an instrumental error in the spectral changes observed in Figure 7(a) and (b).

To further ensure that the sensitivity factor and the surface density previously determined did not influence the spectral behavior obtained for the molar absorptivity reported in Figure 7(a) and (b), we evaluated the ratio of the second derivative of

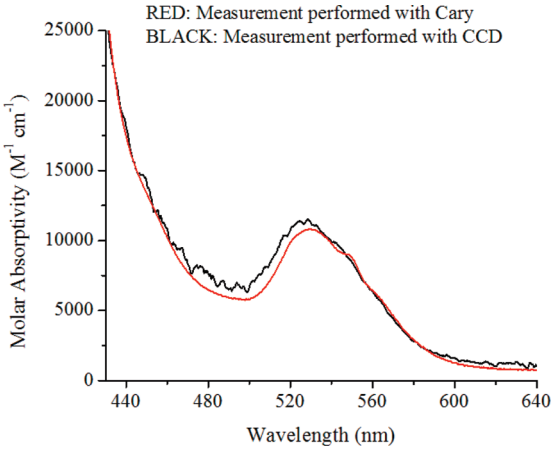

Figure 8. Molar absorptivity for cyt *c* in solution of 10 μM cytochrome *c* in buffer solution (7 mM phosphate, 10 mM NaCl, pH 7.2). The black curve was obtained by placing the 1 cm cuvette in the optical path of our waveguide-based spectrometer, and the red curve was acquired using a commercial UV−vis spectrophotometer.

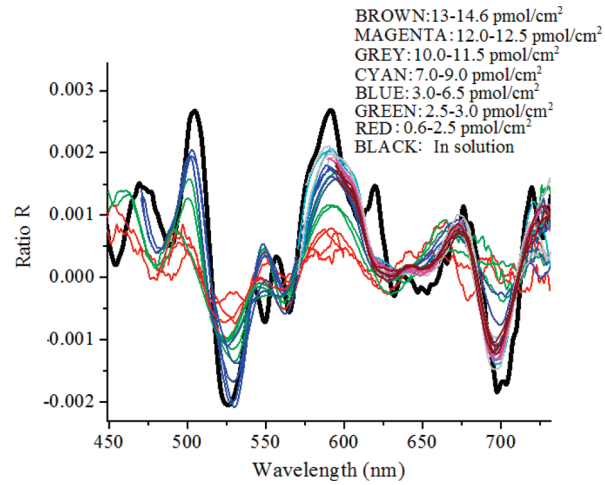

Figure 9. Ratio of the second derivative of the molar absorptivity with respect to the wavelength divided by the molar absorptivity. The quantity *R* in the *y*-axis is independent of the sensitivity factor and surface density calculated for the waveguide. Therefore, it can directly address if a particular transition band is changing its spectral behavior.

the molar absorptivity with respect to the wavelength divided by the molar absorptivity itself. We called this ratio *R*, which then is described by the following equation:

$$R = \frac{\partial^2 \varepsilon_{surf}/\partial\lambda^2}{\varepsilon_{surf}} \cong \frac{\partial^2\left(\frac{A_{WG,TE}}{S_{TE}\Gamma}\right)/\partial\lambda^2}{\frac{A_{WG,TE}}{S_{TE}\Gamma}} = \frac{\partial^2 A_{WG,TE}/\partial\lambda^2}{A_{WG,TE}} \quad (7)$$

In the calculation of the second derivative of the molar absorptivity with respect to the wavelength, the contribution from the inverse of the sensitivity factor was not considered because its value is 3 orders of magnitude smaller than the absorbance term (notice in Figure 2 that the curvature of S_{TE} is fairly constant for wavelengths larger than 450 nm). Therefore, the variable *R* is independent of the previously calculated quantities (sensitivity factor and surface density), is directly related to the measured absorbance data, and gives an unambiguous assessment of the spectral behavior of the adsorbed molecules under investigation. As described in eq 7, changes in *R* with respect to the wavelength represent changes in the curvature of a particular transition band. In Figure 9, the ratio *R* is plotted against the wavelength for both our waveguide-based measurements of surface-adsorbed and solution dissolved cyt *c*. As observed in Figure 9, at low surface coverage of the surface-adsorbed species, the values of *R* are distant from those measured in solution, and at higher surface concentrations, they approach those values from the protein in solution. These results follow exactly the same spectral behavior shown in Figure 7(a) and (b) for the molar absorptivity, so the previously calculated sensitivity and surface densities appear to be valid. Most importantly, the reported data seem to indicate a clear spectral change in the molar absorptivity of cyt *c* under adsorption to the waveguide alumina surface.

In summary, some significant spectral changes in the molar absorptivity values for the Q-band were observed at low surface packing densities (red and green curves in Figure 7(a). When compared to the results obtained in solution, the peak of the molar absorptivity is lower and the transition band has been broadened. The spectral changes in the Q-band described here for surface-adsorbed cyt *c* are consistent with acid denaturation of cytochrome *c*, as already reported in the literature.[18,19,34] During the adsorption process on the waveguide surface, some intramolecular rearrangements may take place at low packing densities in which cytochrome *c* adopts an extended conformation to form more bonds with the surface and maximize the occupied area. However, at higher packing densities, lateral intermolecular interactions between adsorbed proteins may inhibit/reverse this conformational change.[5]

The charge transfer band has long been hailed as a marker of the integrity of the Fe−S bond of cytochrome *c*[34] and, thus, a probe for protein conformational changes.[20] However, it is too weak for conventional instrumentation to corroborate the aforementioned changes in the Q-band. We observed that at low surface coverage (below 3 pmol/cm^2), the peak in the 695 nm region is absent, because we obtained an almost flat curve for the molar absorptivity. When increasing the surface density up to 11 pmol/cm^2, the values tend to approximate those from the protein in solution, but at surface densities higher than 11 pmol/cm^2, where the waveguide surface becomes fully covered, the magenta and brown curves in Figure 7(b), the molar absorptivity starts to deviate again from the corresponding values measured in solution. These data indicate further conformational changes in adsorbed cytochrome *c* that are concentration-dependent, even on an apparently saturated waveguide surface. It should be noted that the maximum packing density observed in these studies, (15 ± 1) pmol/cm^2, is less than the theoretical maximum packing density of 22 pmol/cm^2 sterically allowed for cytochrome *c* on the basis of crystallographic dimensions of the protein.[32]

4. Conclusions

Absorbance measurements were obtained for surface-bound cytochrome *c* onto an alumina surface using a single-mode, integrated optical waveguide spectrometer. Due to the high sensitivity of our instrument, the charge transfer band was measured for a submonolayer of cytochrome *c*, which, to our knowledge, is the first time. In addition, the high sensitivity of our single-mode waveguide-based spectrometer allowed us to experimentally determine the spectral profile of the molar absorptivity for different surface densities; our results show clear spectral changes at low surface densities (below 3 pmol/cm^2).

Under the neutral pH and room temperature conditions of the bulk solution employed in this study, our data shows that

cytochrome *c* adsorbs to the alumina surface with an affinity of $K_{ad} = (10 \pm 2) \times 10^6\ M^{-1}$ and appears to form a monolayer of packing density of 15 pmol/cm^2. The molar absorptivity was calculated for surface densities from 0.3 to 15 pmol/cm^2. At surface densities of subsaturating levels (i.e. below 3 pmol/cm^2), significant spectral changes were observed in the Q and CT bands. These spectral shifts are attributed to surface-induced conformational changes upon adsorption of the protein. Changes in the CT band indicate that the integrity of the $Fe_{Heme}-S_{Met}$ bond is being challenged by these conformational shifts. Shifts in the Q-band indicate a conformational change in the largely hydrophobic heme-binding pocket of cytochrome *c*. Further studies conducted at variable bulk solution conditions (ionic strength, pH, etc.) and comparison of the resulting data with the relative wealth of solution and studies on cytochrome *c* may provide additional information on the exact nature of these conformational changes.

Other ongoing work in our group is aimed at addressing the interaction of proteins with a variety of surfaces and interfaces by exploring the unprecedented sensitivity and broadband capability of our single-mode, integrated optical waveguide spectroscopic technique. Those studies may play an important role in elucidating several molecular monolayer phenomena with potential relevance in many surface and thin-film technologies.

Acknowledgment. The authors acknowledge support from National Institute of Health, Grant no. RR022864-01, and National Science Foundation, Grant no. DBI0359442. We thank Jason Payne for his assistance in this work.

References and Notes

(1) Quinn, A.; Mantz, H.; Jacobs, K.; Bellion, M.; Santen, L. *Europhys. Lett.* **2008**, *81*, 56003.
(2) Lu, M.; Choi, S.; Wagner, C. J.; Eden, J. G.; Cunningham, B. T. *Appl. Phys. Lett.* **2008**, *92*, 261502.
(3) Xu, W. S.; Regnier, F. E. *J. Chromatogr., A* **1998**, *828*, 357.
(4) Yaseen, M.; Salanciski, H. J.; Seifalian, A. M.; Lu, J. R. *Biomed. Mater.* **2008**, *3*, 034123.
(5) Ramsden, J. J. *Phys. Rev. Lett.* **1993**, *71*, 295.
(6) Tie, Y.; Calonder, C.; Van Tassel, P. R. *J. Colloid Interface Sci.* **2003**, *268*, 1.
(7) Fernandez, A.; Ramsden, J. J. *J. Biol. Phys. Chem.* **2001**, *1*, 81.
(8) Malmsten, M. *Biopolymers at Interface*; Marcel Dekker: New York, 2003.
(9) Kato, K.; Takatsu, A.; Matsuda, N.; Azumi, R.; Matsumoto, M. *Chem. Lett.* **1995**, 437.
(10) Mendes, S. B.; Li, L. F.; Burke, J. J.; Lee, J. E.; Dunphy, D. R.; Saavedra, S. S. *Langmuir* **1996**, *12*, 3374.
(11) Matsuda, N.; Takatsu, A.; Kato, K. *Chem. Lett.* **1996**, 105.
(12) Bradshaw, J. T.; Mendes, S. B.; Saavedra, S. S. *Anal. Chem.* **2002**, *74*, 1751.
(13) Mendes, S. B.; Saavedra, S. S. *Opt. Express* **1999**, *4*, 449.
(14) Mendes, S. B.; Li, L. F.; Burke, J. J.; Lee, J. E.; Saavedra, S. S. *Appl. Opt.* **1995**, *34*, 6180.
(15) Mendes, S. B.; Li, L. F.; Burke, J.; Saavedra, S. S. *Opt. Commun.* **1997**, *136*, 320.
(16) Mendes, S. B.; Saavedra, S. S. *Appl. Opt.* **2000**, *39*, 612.
(17) Margoliash, E.; Frohwirt, N. *Biochem. J.* **1959**, *71*, 570.
(18) Droghetti, E.; Smulevich, G. *J. Biol. Inorg. Chem.* **2005**, *10*, 696.
(19) Zucchi, M. R.; Nascimento, O. R.; Faljoni-Alario, A.; Prieto, T.; Nantes, I. L. *Biochem. J.* **2003**, *370*, 671.
(20) Schweitzer-Stenner, R.; Shah, R.; Hagarman, A.; Dragomir, I. *J. Phys. Chem. B* **2007**, *111*, 9603.
(21) Horecker, B. L.; Kornberg, A. *J. Biol. Chem.* **1946**, *165*, 11.
(22) Horecker, B. L.; Stannard, J. N. *J. Biol. Chem.* **1948**, *172*, 589.
(23) Schejter, A.; Aviram, I. *Biochemistry* **1969**, *8*, 149.
(24) Santos, J. H.; Matsuda, N.; Qi, Z. M.; Yoshida, T.; Takatsu, A.; Kato, K. *Anal. Sci.* **2003**, *19*, 199.
(25) Edmiston, P. L.; Lee, J. E.; Cheng, S. S.; Saavedra, S. S. *J. Am. Chem. Soc.* **1997**, *119*, 560.
(26) Kraning, C. M.; Benz, T. L.; Bloome, K. S.; Campanello, G. C.; Fahrenbach, V. S.; Mistry, S. A.; Hedge, C. A.; Clevenger, K. D.; Gligorich, K. M.; Hopkins, T. A.; Hoops, G. C.; Mendes, S. B.; Chang, H. C.; Su, M. C. *J. Phys. Chem. C* **2007**, *111*, 13062.
(27) Babul, J.; Stellwagen, E. *Biochemistry* **1972**, *11*, 1195.
(28) Bradshaw, J. T.; Mendes, S. B.; Saavedra, S. S. *Anal. Chem.* **2005**, *77*, 28A.
(29) Hayes, C. M.; Pereira, M. B.; Brangers, B. C.; Aslan, M. M.; Wiederkehr, R. S.; Mendes, S. B.; Lake, J. H. *Proc. 17th IEEE Univ. Gov. Ind. MicroNano Symp. (UGIM2008)* **2008**, *1*, 227.
(30) Runge, A. F.; Rasmussen, N. C.; Saavedra, S. S.; Mendes, S. B. *J. Phys. Chem. B* **2005**, *109*, 424.
(31) Shah, R.; Schweitzer-Stenner, R. *Biochemistry* **2008**, *47*, 5250.
(32) Runge, A. F.; Rasmussen, N. C.; Saavedra, S. S.; Mendes, S. B. *J. Phys. Chem. B* **2005**, *109*, 424.
(33) Collinson, M.; Bowden, E. F. *Langmuir* **1992**, *8*, 2552.
(34) Scott, R. A.; Mauk, A. G. *Cytochrome c: A Multidisciplinary Approach*; University Science Books: Sausalito, CA, 1996.

JP810845E